

## The comparative studies of HF CVD diamond films by Raman and XPS spectroscopies



Kazimierz Paprocki<sup>a,\*</sup>, Adam Dittmar-Wituski<sup>b</sup>, Marek Trzciński<sup>b</sup>, Mirosław Szybowicz<sup>c</sup>, Kazimierz Fabisiaak<sup>a</sup>, Anna Dychalska<sup>c</sup>

<sup>a</sup> Institute of Physics, Kazimierz Wielki University, Powstańców Wielkopolskich 2, 85-090, Bydgoszcz, Poland

<sup>b</sup> Institute of Mathematics and Physics, University of Science and Technology, ul. Kaliskiego 7, 85-796, Bydgoszcz, Poland

<sup>c</sup> Faculty of Technical Physics, Poznań University of Technology, Piotrowo 3, 60-965, Poznań, Poland

### ARTICLE INFO

**Keywords:**

CVD diamond

Laser Raman spectroscopy

XPS

### ABSTRACT

One of the most attractive features of diamond is its robust p-type surface conductivity that develops under atmospheric conditions on hydrogen-terminated samples. The as-grown CVD diamond films are H-terminated and H concentration depends on the ratios of  $sp^2/sp^3$  carbon bonding. It is well known that the  $sp^2/sp^3$  ratios in CVD diamond films is the key factor determining their physical properties and especially their electrical properties therefore the proper determination of the phase composition of CVD diamond films appear as a very important problem.

The article presents results for seven diamond synthesized by HF CVD method layers analyzed by Scanning Electron Microscopy (SEM), laser Raman spectroscopy (LRS) and X-ray photoelectron spectroscopy (XPS). Values for the ratio of  $sp^2/sp^3$  bonded carbon in the various films were obtained using XPS and LRS methods.

### 1. Introduction

The growing interest in diamond structure continuously increases due to recent progress in chemical vapor deposition (CVD) growth of good quality diamond films [1].

Due to its excellent physical and chemical properties, diamond is considered as an electronic material because of its high Johnson and Keyes Figures of merit values [2]. The physical properties, as for example electrical and optical properties, of CVD diamond films strongly depend on the film preparation conditions.

It is known that "as-grown" diamond layers grown by hot filament chemical vapor deposition (HF CVD) can contain high hydrogen concentrations up to  $10^{19} \text{ cm}^{-3}$  for polycrystalline diamond with micrometer range grain size and up to  $10^{21} \text{ cm}^{-3}$  for nanocrystalline layers.

The diamond microcrystalline films are highly defective, due to grain boundaries or intra-grain dislocations, intergranular amorphous or graphitic regions and hydrogen is supposed to be trapped on these intra- or intergranular defects. The presence of disordered hydrogenated  $sp^2$  carbon in grain boundaries, a high density of dislocations which may trap hydrogen, together with the presence of  $H_2^*$  dimers, are supposed to explain the high hydrogen concentration which can be observed in polycrystalline diamond [3,4]. The diamond film structure

and grain size depend on the growth technique and parameters of CVD growth process.

The XPS method has been recognized since a long time as suitable technique to characterize the surface of diamond films [5] although it remains a very difficult to use because of following reasons:

- difficulty of calibrating the energy scale in the case of insulating or semiconducting materials. For this reason the reported in the literature values of binding energies are ranging from 283.3 to 285.0 eV or even more [5–7].
- in the case of CVD diamond films it is not possible to use the standard cleaning procedure i.e. ion sputtering or annealing because of possibility of surface damage, incorporation of argon ions and also the irreversible transformation of  $sp^3$  carbon atoms into  $sp^2$  carbon bonds [8].
- XPS is a surface sensitive technique, the XPS spectrum could contain also an undesired information on adsorbed elements or additional termination process which can occur during cooling down of diamond films on the end of growth process.

The Raman spectroscopy provides a fast, non-destructive means of characterizing carbon materials, especially CVD diamond film which

\* Corresponding author.

E-mail address: [paprocki@ukw.edu.pl](mailto:paprocki@ukw.edu.pl) (K. Paprocki).

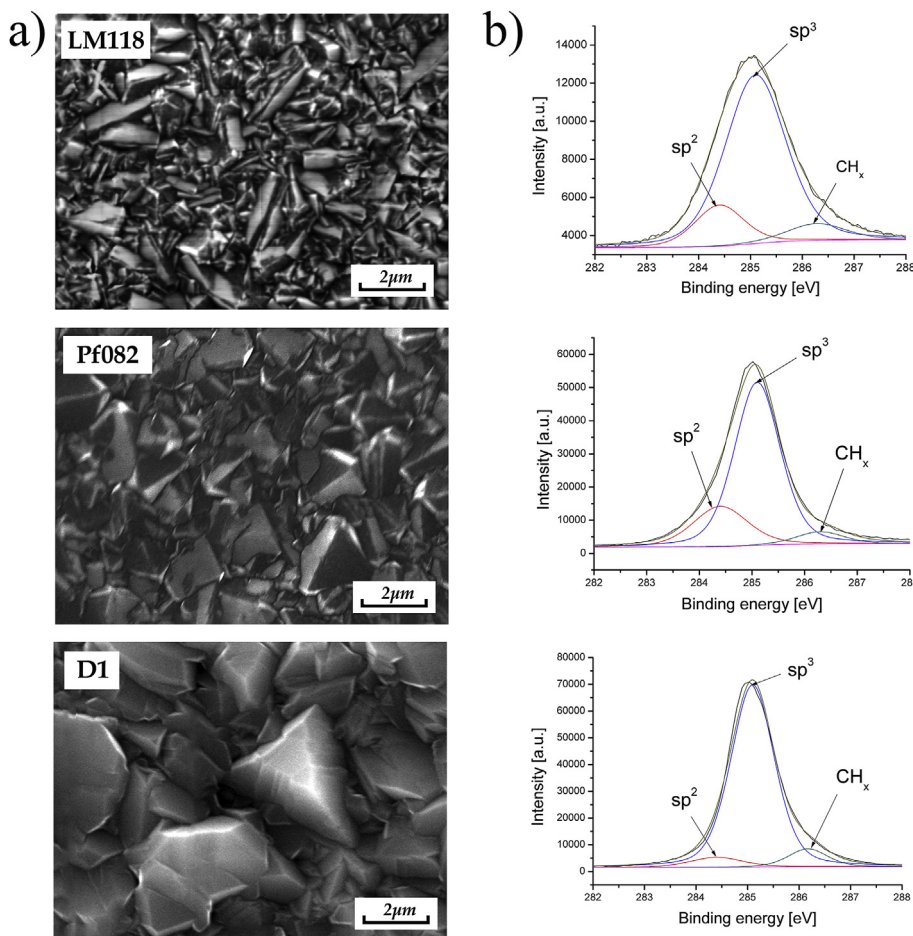


**Fig. 1.** The examples of the results obtained in the performed studies: a) morphology and b) XPS C1s, fitted spectra using three-curve method to find components: sp<sup>3</sup>, sp<sup>2</sup> and CH<sub>x</sub>.

allows for evaluating their quality. The Raman spectra of sp<sup>3</sup> (diamond) and sp<sup>2</sup> (graphitic) hybridized carbon are quite different therefore it is possible to determine the purity of samples as well evaluate the quantity of crystallites or grain boundaries.

Pure diamond has a very simple Raman spectrum, with a single sharp peak at 1332 cm<sup>-1</sup> corresponding to the vibration of the sp<sup>3</sup> diamond lattice. Graphitic carbon gives rise to two peaks, each attributed to ring vibrations.

The relative intensities of these vibrations vary depending on the crystallinity. The “G” peak occurs in the range of 1500–1580 cm<sup>-1</sup> [9] and corresponds to neighboring atoms moving in opposite directions perpendicular to the plane of the graphitic sheet. The “D” peak occurs at 1350 cm<sup>-1</sup> and corresponds to atoms moving in radial directions in the plane of the graphitic sheet, similar to the breathing mode in benzene. The “D” peak appears as a result of dislocations in the lattice, deriving its name from the fact that they are “disorder-induced modes”. As a result, the intensity of this peak relative to the “G” peak can be used to determine the degree of disorder in the sample.

In the case of polycrystalline diamond, the Raman spectra include contributions from both sp<sup>3</sup> and sp<sup>2</sup> carbon. The ratio of the intensity of the diamond peak to the intensity of the “G” peak can be used to estimate the sp<sup>2</sup>/sp<sup>3</sup> ratio help to optimize synthetic conditions [10].

The ratio of sp<sup>2</sup>/sp<sup>3</sup> was also estimated from X-ray photoelectron spectroscopy (XPS) measurements and compared with that obtained from Raman spectroscopy.

## 2. Materials and methods

### 2.1. Samples preparation

The diamond films were grown at the rate of 0.2 μm/h on ultrasonically cleaned, monocrystalline n-Si wafers ((10 x 10) mm, 0.2 mm thickness) as substrates by HF CVD technique. The stainless-steel chamber was water-cooled. The total pressure during growth was 80 mbar. Deposition was carried out using methanol as the carbon containing gas, diluted in H<sub>2</sub>. The total gas flow rate was fixed at the 100 sccm and the percentage flows for methanol vapor and H<sub>2</sub> were changed from 2.3 to 3 vol%. Prior to growth, the substrates were seeded with 1 μm diamond powder in an ultrasonic bath. The growth temperature was estimated to be ~750 °C. Further details of the deposition system are available from an earlier publication [11].

### 2.2. Raman spectroscopy

The Raman spectra were recorded at room temperature in back scattering geometry using Renishaw in Via Raman spectrometer. All spectra were recorded with 488 nm excitation wavelength generated by tunable ion argon laser. The Raman scattering spectra were investigated in the spectral range of 1000–2000 cm<sup>-1</sup>. All data collection was analyzed using Renishaw WiRE 3.1 software using curve fitting method.

### 2.3. Scanning Electron Microscopy

The diamond film morphology, grain's sizes and film thicknesses

have been studied by Scanning Electron Microscope (SEM), Jeol JSM-820 operating at a voltage of 25 kV, using LaB6 Denka cathode.

#### 2.4. XPS

The XPS measurements were performed in UHV system at base pressure =  $2 \times 10^{-10}$  mbar. AlK $\alpha$  (1486.6 eV) nonmonochromatized radiation was used as an excitation source. Photoelectron spectra were obtained by using a VG Scienta R3000 hemispherical analyzer with energy step set to  $\Delta E = 50$  meV. The charge effect was not neutralized, the data was calibrated using O1s (532 eV) line as a reference. Deconvolution of C1s peak was performed by using CasaXPS® software and fitting to Gaussian-Lorentzian profile. The subtracted background was of "Shirley" type.

### 3. Results

In order to show that the LRS and XPS methods can give qualitatively similar results for estimation of  $sp^2/sp^3$  ratio the XPS and LRS measurements were performed on series of 8 CVD diamond films of different qualities and morphologies.

In Fig. 1 are presented examples of SEM pictures of three selected diamond layers together with their corresponding XPS C1s core level spectra. The SEM pictures point to the variability of surface morphology of investigated samples. It is clearly seen that morphological differences are connected mainly with averages grain sizes of about 1  $\mu\text{m}$  for LM118 sample and above 2  $\mu\text{m}$  for D1 sample.

The XPS C1s core-level spectra of CVD diamond films are displayed on right side of the corresponding SEM picture. For each spectrum the phase separation range are also displayed. The C1s peaks are centered on  $\sim 285.1$  eV in all films. A slight widening of the C1s peak is also observed as the morphology is changing. This widening of the C1s peak is accompanied by an increase of its components' intensities in the low as well as in the high energy ranges. Fig. 2a shows corresponding Raman spectra for the samples from Fig. 1. An example of deconvolution of the Raman spectra is shown in Fig. 2b.

The aim of XPS measurements is to investigate the bonding environments of the deposited CVD diamond films. The shape of C1s peak of all samples indicates on the presence of several components including diamond (or  $sp^3$ -hybridized carbon) species, graphitic ( $sp^2$ -hybridized C-C bonds) species and, to a less variable extent component containing hydrogen–carbon bonds.

In order to estimate  $sp^3$  and  $sp^2$  fractions present in the films, we have deconvoluted the C1s peaks into three components of a mixture of 70%:30% of Gaussian and Lorentzian peaks after subtracting the background from the spectra.

Considering the fitting of the data in Fig. 1b, the most intense peak centered at 285.1 eV, may be attributed to the bulk diamond component ( $sp^3$  C–C) with possible contribution from  $sp^3$  CH<sub>1</sub> bonds [12,13]. The less intense component, shifted by about  $-0.7$  eV with respect to diamond peak, might be assigned to graphitic carbon species ( $sp^2$  C–C) [14] and, finally, the least intense peak shifted by  $+1.2$  eV with respect to the  $sp^3$  peak corresponds to CH<sub>x</sub> bonds (where  $x \geq 2$ ) [15].

The deconvolution of C1s peaks shown in Fig. 1b allows to determine the ratios of  $sp^2/sp^3$  using the ratio of surface area  $A_{sp^2}$  under  $sp^2$  peak to the surface  $A_{sp^3}$  under  $sp^3$  peak:

$$sp^2/sp^3 = A_{sp^2}/A_{sp^3} \quad (1)$$

The ratio  $sp^2/sp^3$  and FWHM value C1s peak of the diamond films were found to be dependent, at first look, on the morphology and especially on the microcrystalline sizes in the diamond films.

The ratio  $sp^2/sp^3$  can be also determined by Raman spectroscopy from the  $1332\text{ cm}^{-1}$  diamond peak ( $sp^3$ ) and the  $sp^2$  from  $1550\text{ cm}^{-1}$  G band. Hydrogen concentration appears to be proportional to the  $sp^2$  bonds ratio [16]. It was also shown that the H concentration is

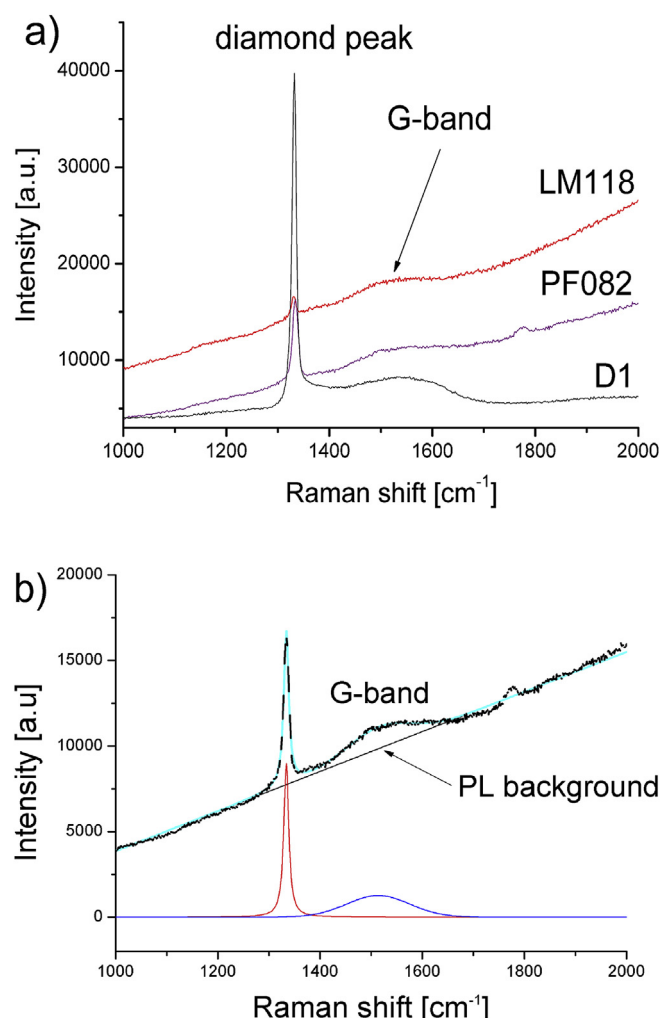


Fig. 2. a) The Raman spectra of the samples shown in Fig. 1, b) the deconvoluted Raman spectrum of PF082 sample.

proportional to the slope of photoluminescence background of the Raman spectrum according to simple quantitative formula given by C. Casiraghi et al. [17].

$$H[\text{at.\%}] = 21.7 + 16.6 \log\{m/I_G [\mu\text{m}]\} \quad (2)$$

where: m-is the slope of photoluminescence background of the Raman spectrum in the units of  $\mu\text{m}$ ,  $I_G$ -is the integral intensity of the G band in Raman spectrum.

Examples of the Raman spectra corresponding to the diamond films shown in Fig. 1a are presented in Fig. 2b. The parameters of XPS and Raman spectra for above samples are listed in Table 1 and Table 2 respectively.

As it is seen from Fig. 2b all Raman spectra are characterized by sharp diamond Raman peak at  $\sim 1331.9\text{ cm}^{-1}$  and broad G-band at around  $1500\text{--}1530\text{ cm}^{-1}$ . It is also clearly seen that above Raman spectra show different slope of photoluminescence background indicating on different H concentration.

The method of the  $sp^2/sp^3$  estimation from Raman spectroscopy measurements was described in our earlier work [11].

### 4. Discussion

The fitting procedure of C1s peak assumed that it consist of three peaks, the  $sp^3$  peak, the  $sp^2$  peak and CH<sub>x</sub> peak. The shapes of above peaks was assumed to be a mixture of Gaussian and Lorentzian peaks.

**Table 1**

The parameters of XPS spectra.

Sample	CH <sub>3</sub> OH [vol%]	FWHM of individual peaks [eV]				Percentage of individual peaks [%]			The ratio of sp <sup>2</sup> /sp <sup>3</sup>
		C1s	sp <sup>2</sup>	sp <sup>3</sup>	CH <sub>x</sub>	sp <sup>2</sup>	sp <sup>3</sup>	CH <sub>x</sub>	
LM14	3.0	1.917	1.192	1.389	1.559	12.49	61.87	20.64	0.200
LM118	2.9	1.808	1.174	1.379	1.348	11.26	72.64	16.10	0.155
PF070	2.7	1.385	1.184	1.182	1.256	10.48	82.91	6.61	0.127
PF082	2.6	1.325	1.217	1.020	1.049	8.56	84.55	6.89	0.104
DPK19	2.5	1.201	1.287	1.069	1.027	9.47	85.93	4.60	0.110
DPK35	2.4	1.075	1.234	1.092	1.012	7.18	88.51	4.31	0.080
D1	2.3	1.057	1.187	0.990	0.887	4.69	91.21	4.10	0.051

The peak height of the sp<sup>3</sup> and sp<sup>2</sup> peaks and the CH<sub>x</sub> peak position were allowed to vary for a best fit to the experimental data. The examples of XPS spectra deconvolution are shown in Fig. 1b. The best fits of XPS spectra showed that the energy separations between sp<sup>3</sup>, sp<sup>2</sup> and CH<sub>x</sub> peaks for all samples reached the same, constant values equal  $\Delta E_{\text{sp}^3-\text{sp}^2} = 0.7 \text{ eV}$  and  $\Delta E_{\text{sp}^3-\text{CH}_x} = 1.2 \text{ eV}$ .

The number of carbon atoms in each hybridization is proportional to the area under each peak. It is especially interesting to calculate sp<sup>2</sup>/sp<sup>3</sup> ratio from XPS spectra and compare the obtained results with results derived from Raman spectroscopy measurements. Fig. 3a shows the correlation of the two methods.

The ratio of sp<sup>2</sup>/sp<sup>3</sup> estimated by these two independent methods give qualitatively compatible results i.e. are proportional to each other. The differences may be due to the fact that XPS is a surface method (the signal originates from depths 1-2 nm) and Raman spectroscopy is a rather bulk method.

As mentioned earlier the slope of the PL background in Raman spectrum may originate from hydrogen atoms chemically bonded to amorphous carbon phase (sp<sup>2</sup> hybridized carbon phase admixture). Fig. 3b presents the correlation between CH<sub>x</sub> fraction estimated from XPS and slope „m” of PL background of Raman spectrum.

The correlation shown in Fig. 3b confirms that the main source of the luminescent background may be hydrogen bonded chemically (CH<sub>x</sub> bonds) to the carbon atoms on diamond surface.

The nonlinearity of this relation may arise from the nature of clustering mechanism of sp<sup>2</sup> bonded carbon phase which is still not fully explained. According to amorphization trajectory developed by Ferrari et al. [9], it is known that the increasing clustering lowers the Raman G-band position and decreases its FWHM what was also observed for our samples (see Table 1).

The sizes of sp<sup>2</sup> clusters has an influence the level of diamond H-terminated surface and also on the amount of CH<sub>x</sub> bonds as it is indicated by value of the slope m of the PL background in Raman spectra. The diamond layers with bigger diamond microcrystal (Fig. 1 sample D1) reveal mostly the 3-D character while surface of the sample LM118 (Fig. 1) is much more flat and has rather 2-D character. Nonlinear behavior shown in Fig. 3b (also relation shown in Fig. 4) may arise therefore from the geometrical effect.

As it is shown in Fig. 1b and Table 1 the XPS core level C1s spectra of CVD diamond layer can be characterized by different values of

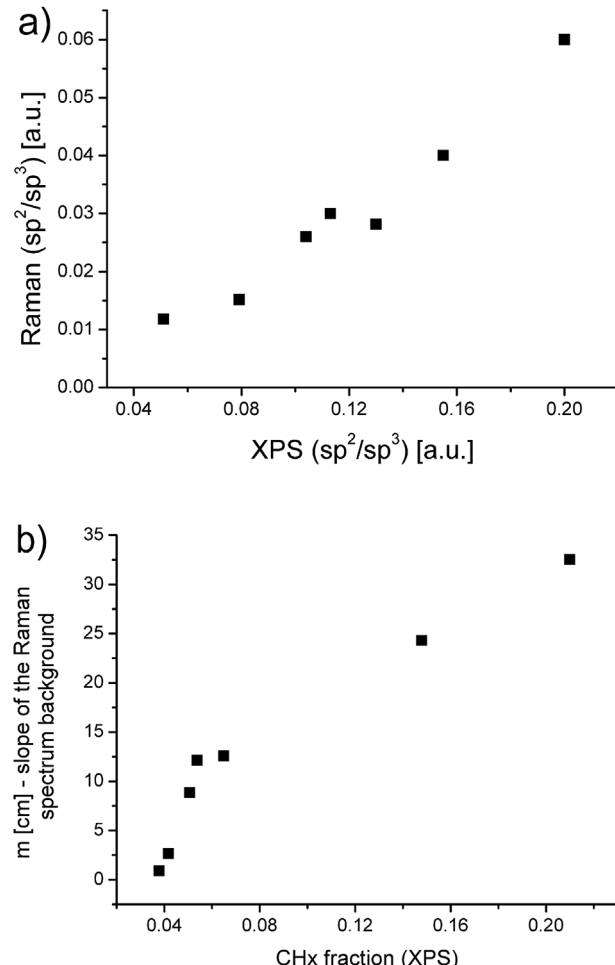


Fig. 3. a) The correlation between sp<sup>2</sup>/sp<sup>3</sup> ratios estimated from Raman and XPS spectroscopy measurements, b) The dependence of the slope „m” vs. CH<sub>x</sub> fraction.

**Table 2**

The parameters of Raman spectra.

Sample	CH <sub>3</sub> OH [vol%]	Diamond peak position [cm <sup>-1</sup> ]	FWHM Raman sp <sup>3</sup> [cm <sup>-1</sup> ]	G-band Raman peak [cm <sup>-1</sup> ]	FWHM G-band [cm <sup>-1</sup> ]	The ratio of sp <sup>2</sup> /sp <sup>3</sup>	Slope m of PL background [cm]
LM14	3.0	1331.8	9.18	1500	99.3	0.061	32.40
LM118	2.9	1331.1	9.60	1503	112	0.042	24.34
PF070	2.7	1331.6	9.70	1516	139	0.028	12.50
PF082	2.6	1332.7	11.60	1515	145	0.031	12.10
DPK19	2.6	1331.8	10.50	1533	178	0.025	8.50
DPK35	2.4	1332.3	9.90	1538	185	0.016	1.05
D1	2.3	1332.1	9.40	1531	252	0.012	2.50

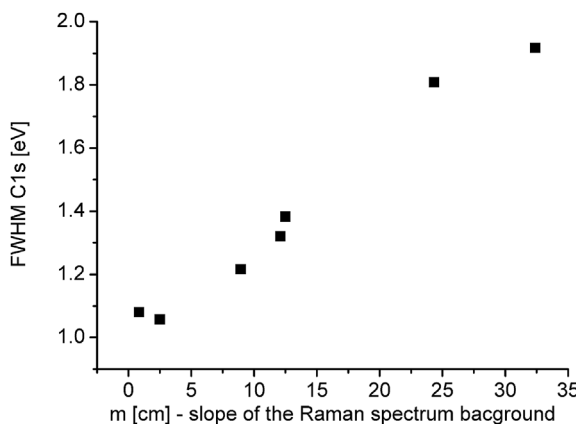


Fig. 4. FWHM of C1s XPS spectrum vs. slope „m”.

FWHM. It is well known that FWHM of C1s peak for diamond or graphite is much smaller in comparison to value of FWHM observed in case of amorphous carbon films [18].

In the case of a-C:H it is assumed that the C1s spectra consist of both  $sp^3$  and  $sp^2$  configurations of carbon, the C1s peak may consist of two groups of C1s photoelectrons, one from carbon atoms in the  $sp^3$ -hybridized and the other from the  $sp^2$  hybridized carbon bonds and possible admixture of  $CH_x$  bonds. Relative concentrations of above type of bonding determine the value of FWHM of C1s core level XPS peak. The same situation may occur in the case of CVD diamond layer which contain some admixture of amorphous carbon phase. In Fig. 4 we present the correlation between slope „m” of PL background vs. FWHM of C1s XPS spectrum.

From Fig. 4 one may conclude that the widening of C1s XPS spectra was caused by chemically bonded hydrogen which concentration is determined by slope m of PL background of Raman spectrum.

On the other hand, Fig. 3b indicates that m parameter depends on the  $CH_x$  concentration. Since the separation of XPS peaks for the  $sp^3$  and  $CH_x$  phases is much larger (1.2 eV) than the  $sp^3-sp^2$  separation (0.7 eV), the widening of the FWHM XPS C1 peak is mainly influenced by the  $CH_x$  content.

## 5. Conclusions

Thin polycrystalline diamond films were grown in HFCVD reactor from  $CH_3OH/H_2$  mixture with  $CH_3OH$  concentration in the range of 2.3–3.0 vol%. The variation of methanol concentration in films revealed an influence on their surface properties associated to the morphology and  $sp^2$  hybridized carbon phase contents in the films. The characteristic diamond Raman peaks for all samples are centered approximately at  $1331.9\text{ cm}^{-1}$  with comparable values of FWHM equal to  $10\text{ cm}^{-1}$  in average i.e. show very weak dependence on methanol concentration. The positions and FWHM of the Raman G-bands indicate that  $sp^2$ -hybridized carbon phase undergoes clustering mechanism as methanol addition increases.

The numerical analysis of the Raman and XPS spectra confirmed the increase of  $sp^2$ -hybridized carbon phase in the diamond films as the methanol concentration increases. The estimated values of  $sp^2/sp^3$  ratios using both above methods showed that these values are proportional to each other i.e. gave qualitatively compatible results. The further work is required to achieve also quantitative compliance.

## Acknowledgements

This work was supported in part by Project of Kazimierz Wielki University for development of basic research and by the Ministry of Science and Higher Education within Project realized at Faculty of Technical Physics, Poznan University of Technology No. 06/65/SBAD/1952.

## References

- [1] Q. Liang, Y. Meng, C.-S. Yan, S. Krasnicki, J. Lai, K. Hemawan, H. Shu, D. Popov, T. Yu, W. Yang, Developments in synthesis, characterization, and application of large, high-quality CVD single crystal diamond, *J. Superhard Mater.* 35 (2013) 195–213 <https://doi.org/10.3103/s1063457613040011>.
- [2] H. Shiomi, Diamond active electronic devices, in: J. Asmussen, D.K. Reinhard (Eds.), *Diamond Films Handbook*, CRC Press, 2002, p. 579.
- [3] S. Michaelson, O. Ternyak, R. Akhvlediani, A. Hoffman, A. Lafosse, R. Azria, O.A. Williams, D. Gruen, Hydrogen concentration and bonding configuration in polycrystalline diamond films: from micro-to nanometric grain size, *J. Appl. Phys.* 102 (2007) 113516 <https://doi.org/10.1063/1.2818372>.
- [4] S.A. Rakha, Y. Guojun, C. Jianqing, Correlation between diamond grain size and hydrogen incorporation in nanocrystalline diamond thin films, *J. Exp. Nanosci.* 7 (2012) 378–389 <https://doi.org/10.1080/17458080.2010.529171>.
- [5] J. Wilson, J. Walton, G. Beaman, Analysis of chemical vapour deposited diamond films by X-ray photoelectron spectroscopy, *J. Electron Spectrosc.* 121 (2001) 183–201 [https://doi.org/10.1016/s0368-2048\(01\)00334-6](https://doi.org/10.1016/s0368-2048(01)00334-6).
- [6] J. Filik, P. May, S. Pearce, R. Wild, K. Hallam, XPS and laser Raman analysis of hydrogenated amorphous carbon films, *Diam. Relat. Mater.* 12 (2003) 974–978 [https://doi.org/10.1016/s0925-9635\(02\)00374-6](https://doi.org/10.1016/s0925-9635(02)00374-6).
- [7] L. Demuynck, J. Arnault, R. Polini, F. Le Normand, CVD diamond nucleation and growth on scratched and virgin Si (100) surfaces investigated by in-situ electron spectroscopy, *Surf. Sci.* 377 (1997) 871–875 [https://doi.org/10.1016/s0039-6028\(96\)01501-4](https://doi.org/10.1016/s0039-6028(96)01501-4).
- [8] Y. Fan, A. Fitzgerald, P. John, C. Troupé, J. Wilson, X-ray photoelectron spectroscopy studies of CVD diamond films, *Surf. Interface Anal.* 34 (2002) 703–707 <https://doi.org/10.1002/sia.1392>.
- [9] A. Ferrari, J. Robertson, Resonant Raman spectroscopy of disordered, amorphous, and diamondlike carbon, *Phys. Rev. B* 64 (2001) 075414 <https://doi.org/10.1103/physrevb.64.075414>.
- [10] A. Dychalska, K. Fabisiak, K. Paprocki, J. Makowiecki, A. Iskaliyeva, M. Szybowicz, A Raman spectroscopy study of the effect of thermal treatment on structural and photoluminescence properties of CVD diamond films, *Mater. Des.* 112 (2016) 320–327 <https://doi.org/10.1016/j.matdes.2016.09.092>.
- [11] K. Fabisiak, A. Banaszak, M. Kaczmarski, M. Kozanecki, Structural characterization of CVD diamond films using Raman and ESR spectroscopy methods, *Opt. Mater.* 28 (2006) 106–110 <https://dx.doi.org/10.1016/j.optmat.2004.11.057>.
- [12] D. Balltaud, N. Simon, H. Girard, E. Rzepka, B. Bouchet-Fabre, Photoelectron spectroscopy of hydrogen at the polycrystalline diamond surface, *Diam. Relat. Mater.* 15 (2006) 716–719 <https://doi.org/10.1016/j.diamond.2006.01.004>.
- [13] S. Ghodbane, D. Balltaud, F. Omnes, C. Agnes, Comparison of the XPS spectra from homoepitaxial {111}, {100} and polycrystalline boron-doped diamond films, *Diam. Relat. Mater.* 19 (2010) 630–636 <https://doi.org/10.1016/j.diamond.2010.01.014>.
- [14] N. Dwivedi, S. Kumar, I. Rawal, H.K. Malik, Influence of consumed power on structural and nano-mechanical properties of nano-structured diamond-like carbon thin films, *Appl. Surf. Sci.* 300 (2014) 141–148 <https://doi.org/10.1016/j.apsusc.2014.02.023>.
- [15] A. Azevedo, J. Matsushima, F. Vicentin, M. Baldan, N. Ferreira, Surface characterization of NCD films as a function of  $sp^2/sp^3$  carbon and oxygen content, *Appl. Surf. Sci.* 255 (2009) 6565–6570 <https://doi.org/10.1016/j.apsusc.2009.02.041>.
- [16] D. Balltaud, F. Jomard, T. Kociniewski, E. Rzepka, H. Girard, S. Saada,  $Sp^3/Sp^2$  character of the carbon and hydrogen configuration in micro- and nanocrystalline diamond, *Diam. Relat. Mater.* 17 (2008) 451–456 <https://dx.doi.org/10.1016/j.diamond.2007.10.004>.
- [17] C. Casiraghi, A. Ferrari, J. Robertson, Raman spectroscopy of hydrogenated amorphous carbons, *Phys. Rev. B* 72 (2005) 085401 <https://doi.org/10.1103/physrevb.72.085401>.
- [18] S. Ogawa, R. Sugimoto, N. Kamata, Y. Takakuwa, Decreased hydrogen content in diamond-like carbon grown by  $CH_4/Ar$  photoemission-assisted plasma chemical vapor deposition with  $CO_2$  gas, *Surf. Coat. Technol.* 350 (2018) 863–867 <https://doi.org/10.1016/j.surfcoat.2018.04.016>.